



Article

# Ruellia tuberosa Ethyl Acetate Leaf Extract Induces Apoptosis and Cell Cycle Arrest in Human Breast Cancer Cell Line, MCF-7

Fui Fui Lem , Bo Eng Cheong and Peik Lin Teoh \*

Biotechnology Research Institute, Universiti Malaysia Sabah, Jalan UMS, Kota Kinabalu 88400, Sabah, Malaysia; lemfuifui02@gmail.com (F.F.L.); becheong@ums.edu.my (B.E.C.)

\* Correspondence: peiklin@ums.edu.my; Tel.: +6088-320000; Fax: +6088-320993

**Abstract:** *Ruellia tuberosa* L. has been previously shown to possess antioxidant and antiproliferative activities on cancer cells but its underlying mechanisms are largely unknown. This study aimed to elucidate the mode of action underlying this inhibitory effect on MCF-7 using ethyl acetate extract obtained after liquid-liquid partition of methanol crude extract. Antiproliferative effect of *R. tuberosa* ethyl acetate leaf extract (RTEAL) was evaluated using MTT assay. Its ability to induce apoptosis was assessed by DNA ladder formation, JC-1, Annexin V, and methylene blue staining assays. Perturbation of cell cycle progression was determined using flow cytometry. RTEAL was found to selectively inhibit the proliferation of MCF-7 cells with the IC<sub>50</sub> value of 28 µg/mL. Morphological changes such as nuclear fragmentation and chromatin condensation were observed although DNA laddering was undetected in agarose gel. RTEAL-induced apoptotic pathways by inhibiting the expression of anti-apoptotic BCL-2 while upregulating pro-apoptotic BAX, caspase 7 and caspase 8. RTEAL also caused cell cycle arrests at the S and G2/M phase and dysregulation of cell cycle regulators. These findings collectively demonstrate that RTEAL extract inhibited cell growth by inducing apoptosis and cell cycle arrest, suggesting its therapeutic potential against breast cancer.



**Citation:** Lem, F.F.; Cheong, B.E.; Teoh, P.L. *Ruellia tuberosa* Ethyl Acetate Leaf Extract Induces Apoptosis and Cell Cycle Arrest in Human Breast Cancer Cell Line, MCF-7. *Sci. Pharm.* **2022**, *90*, 44. <https://doi.org/10.3390/scipharm90030044>

Academic Editor: William A. Donaldson

Received: 29 May 2022

Accepted: 8 July 2022

Published: 25 July 2022

**Publisher's Note:** MDPI stays neutral with regard to jurisdictional claims in published maps and institutional affiliations.



**Copyright:** © 2022 by the authors. Licensee MDPI, Basel, Switzerland. This article is an open access article distributed under the terms and conditions of the Creative Commons Attribution (CC BY) license (<https://creativecommons.org/licenses/by/4.0/>).

## 1. Introduction

Despite the advances of targeted therapy, the success of cancer therapy is hampered by individual clinicopathological variables, genetic aberration, as well as undesirable adverse side effects after treatment [1]. Breast cancer becomes the most leading cancer worldwide, overtaking lung cancer in 2021. According to World Health Organization, breast cancer has impacted 2.26 million women worldwide and caused 685,000 deaths in 2020 [2]. Based on molecular characterization, breast cancer is no longer classified as a single disease as its cell growth, progression, and susceptibility to treatments are dictated by the heterogeneity of genetic alterations [3,4]. Therefore, targeting multiple molecular pathways offers a better prospect for achieving long-term success in controlling tumor cell growth, resistance, and metastasis [5,6].

Apoptosis is a programmed cell death that can be activated via extrinsic (receptor-mediated) and intrinsic (mitochondrial-mediated) pathways which are tightly regulated by BCL-2 family members such as BAX, BCL-2 and a group of caspases including caspase 3,7, 8 and 9 [7]. It is crucial in controlling a balance between survival and death of cells. Defective apoptotic pathways and cell cycle machinery are two of the main factors associated with chemoresistance in breast cancer. Thus, chemotherapeutic and chemopreventive agents that can target both mechanisms in cancer cells is desired [7,8]. Plants have a long history in cancer treatment, and more than 60% anticancer drugs approved by the US Food and Drug Administration are plant-based [9,10]. In contrast with current chemotherapy drugs, which mostly act as monotarget molecules, many phytochemicals have been shown to impede cancer growth by modulating multiple mechanisms such as apoptosis and signaling pathways [11,12].

*Ruellia tuberosa* L. is a Minnie root medicinal plant, a tropical plant widely distributed in South East Asia including Sabah, Malaysia. It has been traditionally used as a diuretic, antidiabetic, antipyretic, analgesic and anti-hypersensitive agent [13]. The plant extracts from its stem, leaves and roots also exhibited antioxidant, antimicrobial, antinociceptive, and anti-inflammatory effects [14–17]. Some of the chemical constituents found in this plant are cirsimarin, cirsiliol 4'-glucoside, sorbifolin, pedalitin, betulin, vanillic acid, squalene, lupeol, and phytosterols [17–20]. Our GC-MS analysis showed that this plant contains squalene, lupeol, stigmasterol, vitamin E and campesterol which may work synergically to inhibit cancer cell growth [18]. Some of these compounds have been previously reported to possess anticancer activity [21–23]. In addition, we have also tested that pure compound such as squalene and lupeol could prevent the proliferation of MCF-7 (unpublished data). *R. tuberosa* extracts also exhibited anticancer properties in breast, cervical, lung and liver cancer cells [24,25], but its underlying mechanisms are unclear. The inhibitory effect of *R. tuberosa* extracts on MCF-7 [24] has prompted us to investigate its efficacy after solvent partitioned the methanolic leaf extract. Among the fractions, ethyl acetate leaf extracts (RTEAL) showed the most profound inhibitory effect; thus its mode of action was elucidated in this study.

## 2. Materials and Methods

### 2.1. Plant Material and Extraction

The leaves of *R. tuberosa* were collected from Kingfisher, Kota Kinabalu, Sabah, Malaysia and planted in Biotechnology Research Institute in 2013. The plant specimen was authenticated by a botanist, Mr. Johnny Gisil and of the specimen voucher (ACRT01/2013) was deposited at the herbarium of Universiti Malaysia Sabah. Briefly, fresh leaves were harvested, washed and freeze-dried. The freeze-dried leaves were ground finely into powder and used for extraction. The leaf powder (12 g) was extracted using 300 mL of methanol by using Soxhlet apparatus for 13 h. The extract was concentrated at 40 °C in a rotary evaporator (Buchi, Switzerland) then freeze-dried. Liquid-liquid partitioning of methanolic extracts was performed according to the method described by Teoh et al. [26]. Five grams of dried extracts were dissolved with 125 mL distilled water and partitioned with hexane, chloroform, and ethyl acetate, respectively, with the ratio 1:1. The partitioned extracts were dried using a rotary evaporator and stored in –80 °C until further use. All solvents used in plant extraction were purchased from Fisher Scientific (Leicestershire, UK).

### 2.2. Cell Culture and Treatment

Human breast cancer cell line (MCF-7) and mouse embryonic fibroblast cell line (NIH 3T3) were cultured in RPMI1640 (Nacalai Tesque, Kyoto, Japan) supplemented with 100 U/mL penicillin/streptomycin (Life Technologies, Grand Island, NY, USA) and 10% FBS (J R Scientific, CA, USA). Human mammary epithelial cell line (MCF10A) was maintained in DMEM/F12 medium (Life Technologies, Grand Island, NY, USA) consisting of 5% horse serum (Life Technologies, Grand Island, NY, USA), 10 µg/mL human recombinant insulin (Sigma, St. Louis, MO, USA), 20 ng/mL epidermal growth factor (Pepro-Tech, Cranbury, NJ, USA), 0.5 mg/mL hydrocortisone (Sigma, St. Louis, MO, USA) and 100 U/mL penicillin/streptomycin (Life Technologies, Grand Island, NY, USA). Cell lines were gifts from Dr. Khoo Boon Yin (University of Science Malaysia). All cell lines were maintained at 37 °C in a humidified atmosphere supplied with 5% CO<sub>2</sub>. MCF-7 cells were treated with the respective concentrations as indicated. For camptothecin, the treatment was performed at 0.4 µg/mL for 24 h.

### 2.3. Cell Proliferation Assay

The effect of plant extracts on cell proliferation was performed using MTT Cell Proliferation Kit I (Roche Diagnostics, Mannheim, Germany) according to the manufacturer's protocol. Cells were seeded onto 96-well plate at the density of 5 × 10<sup>3</sup> (MCF-7 and MCF10A) and 1 × 10<sup>4</sup> (NIH3T3) and incubated for 24 h. The cells were treated with RTEAL

at the concentrations ranging from 10–50 µg/mL for 72 h. The optical density was measured at 550 nm using a microplate reader. Half maximal inhibitory concentration ( $IC_{50}$ ) is defined as the plant extract's concentration required for 50% inhibition of cell growth.  $IC_{50}$  value obtained was used for subsequent experiments. Data were obtained from three independent experiments with triplicate for each treatment.

#### 2.4. Cell Staining

For methylene blue, 100 µL of 2% methylene blue (Sigma, St. Louis, MO, USA) was added to the cells and incubated for 10 min at room temperature. After discarding methylene blue, cells were washed with 1× DPBS (Nacalai Tesque, Kyoto, Japan). Nuclear DNA staining was performed using NucBlue Fixed Cell Stain (Life Technologies, Grand Island, NY, USA) according to the manufacturer's protocol. The cell morphological changes were observed using a fluorescence microscope (Olympus, Tokyo, Japan).

#### 2.5. Detection of DNA Ladder

The genomic DNA was extracted using Apoptotic DNA Ladder Kit (Roche Diagnostics, Mannheim, Germany) according to the manufacturer's instruction. DNA was extracted using lysis buffer after incubation for 10 min. The cell lysate was mixed with 100 µL of isopropanol then transferred into a column before centrifugation. Finally, DNA was eluted using elution buffer after washing steps. The formation of DNA ladder was observed by agarose gel electrophoresis. The 1 kB DNA marker used in this study was obtained from Thermo Fisher (Bedford, MA, USA)

#### 2.6. Apoptosis Assay

Apoptotic cells were detected using Tali Apoptosis Kit-Annexin V Alexa Fluor® 488 and propidium iodide (PI) (Life Technologies, Grand Island, NY, USA). Briefly, cell pellet ( $1 \times 10^5$  cells) was resuspended with 100 µL of Annexin V Binding Buffer and 5 µL of Annexin V before incubated for 20 min. After adding 1 µL of propidium iodide, cells were incubated for 5 min. The analysis was carried out using TALI image-based cytometer (Life Technologies, Grand Island, NY, USA).

#### 2.7. Measurement of Mitochondrial Membrane Potential

Measurement of mitochondrial membrane potential was performed using BD™ MitoScreen Kit (BD Biosciences, San Jose, CA, USA). Cells ( $1 \times 10^5$  per well) were seeded onto 6-well plates and processed according to the protocol described in the manufacturer's manual. JC-1 working solution was added into the cells and incubated at 37 °C. After washing with 1× assay buffer, cells were analyzed using flow cytometry FACSaria Flow Cytometry (BD Biosciences, San Jose, CA, USA).

#### 2.8. Cell Cycle Analysis

The cell cycle analysis was performed using BD CycleTest Plus DNA Reagent Kit (BD Biosciences, San Jose, CA, USA) according to manufacturer's protocols. Cells were washed with cold 1× DPBS and stained prior analysis using FACSaria Flow Cytometry (BD Biosciences, San Jose, CA, USA). Flow cytometric data were analyzed using Modfit software version 3.2 (BD Biosciences, San Jose, CA, USA).

#### 2.9. Isolation of RNA and RT-PCR

Total RNA was isolated using RNeasy plus mini kit (Qiagen, Valencia, CA, USA) according to the manufacturer's protocol. RT-PCR was performed using OneStep RT-PCR kit (Qiagen, Valencia, CA, USA). The PCR conditions and primers used in this study was carried out using methods mentioned in Teoh et al. [26].

## 2.10. Protein Extraction and Western Blot Analysis

Protein was extracted and subjected to Western blotting using the method described in Teoh et al. [27]. Protein concentration was quantified using the Qubit protein assay kit (Life Technologies, USA). Antibodies against BAX, BCL-2,  $\beta$ -tubulin, cyclin E1, cyclin A2 and horseradish peroxidase (HRP)-conjugated IgG were obtained from Cell Signaling (Danvers, MA, USA) while CDK2, caspase 7 and caspase 8 were purchased from Abcam (Cambridge, MA, USA). The relative protein expression was quantified after normalization using  $\beta$ -tubulin.

## 2.11. Statistical Analysis

Statistical analysis was performed using one way ANOVA (SPSS version 16 software). Results were expressed as the mean  $\pm$  SEM obtained from three independent experiments. Asterisks indicate a significant difference (\*  $p < 0.05$ ; \*\*  $p < 0.01$ ).

## 3. Results

### 3.1. Antiproliferative Effects of RTEAL

MTT results revealed a concentration-dependent manner of RTEAL on MCF-7. The cancer cell growth was gradually decreased with the concentration (Figure 1). The IC<sub>50</sub> value obtained was 28  $\mu$ g/mL after RTEAL treatment for 72 h. On the other hand, minimal inhibition was observed in NIH3T3, whereas a slight increase in proliferation was observed in MCF-10A cells (Figure 1). This suggests that the antiproliferative effect of RTEAL is selective against MCF-7.

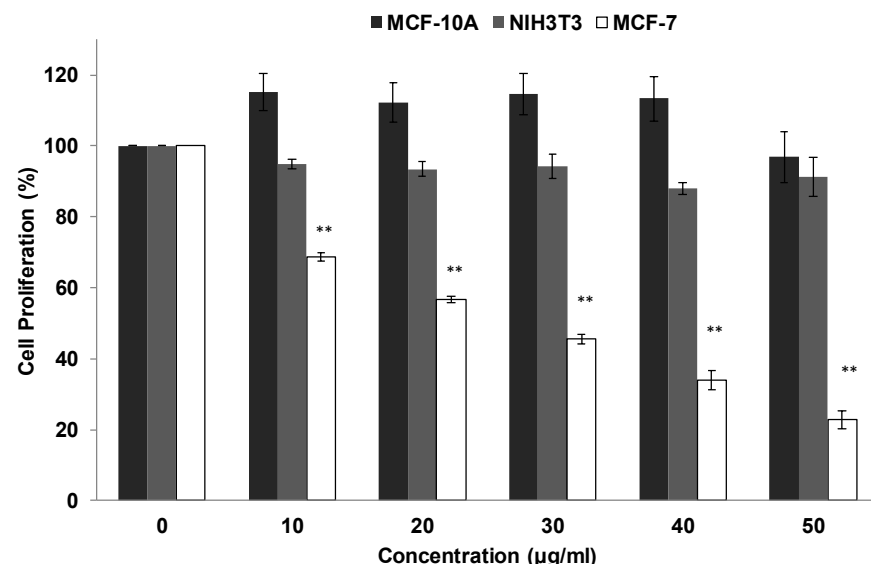


**Figure 1.** Antiproliferative effect of RTEAL on breast cancer cell line. MCF-7, MCF-10A and NIH3T3 cells were treated with RTEAL at the concentrations as indicated for 72 h. The assay was performed using MTT reagent. Data were presented as mean  $\pm$  SEM of the three independent experiments with triplicate for each treatment. Asterisks indicate a significant difference (\*\*  $p < 0.01$ ) for each concentration was compared to the control cells.

### 3.2. Effects of RTEAL on Cell Morphology and DNA Fragmentation

RTEAL-treated cells demonstrated noticeable morphological changes such as nuclear fragmentation, chromatin condensation and appearance of intense DAPI-stained micronuclei (Figure 2A,B) when compared to untreated cells (control). These features were also observed in camptothecin-treated cells. In Figure 2C, a smear of high molecular weight (HMW) DNA was detected in cells treated with RTEAL for 24, 48 and 72 h, but not in the control sample. Nevertheless, we did see the formation of the DNA ladder in cells treated with camptothecin.

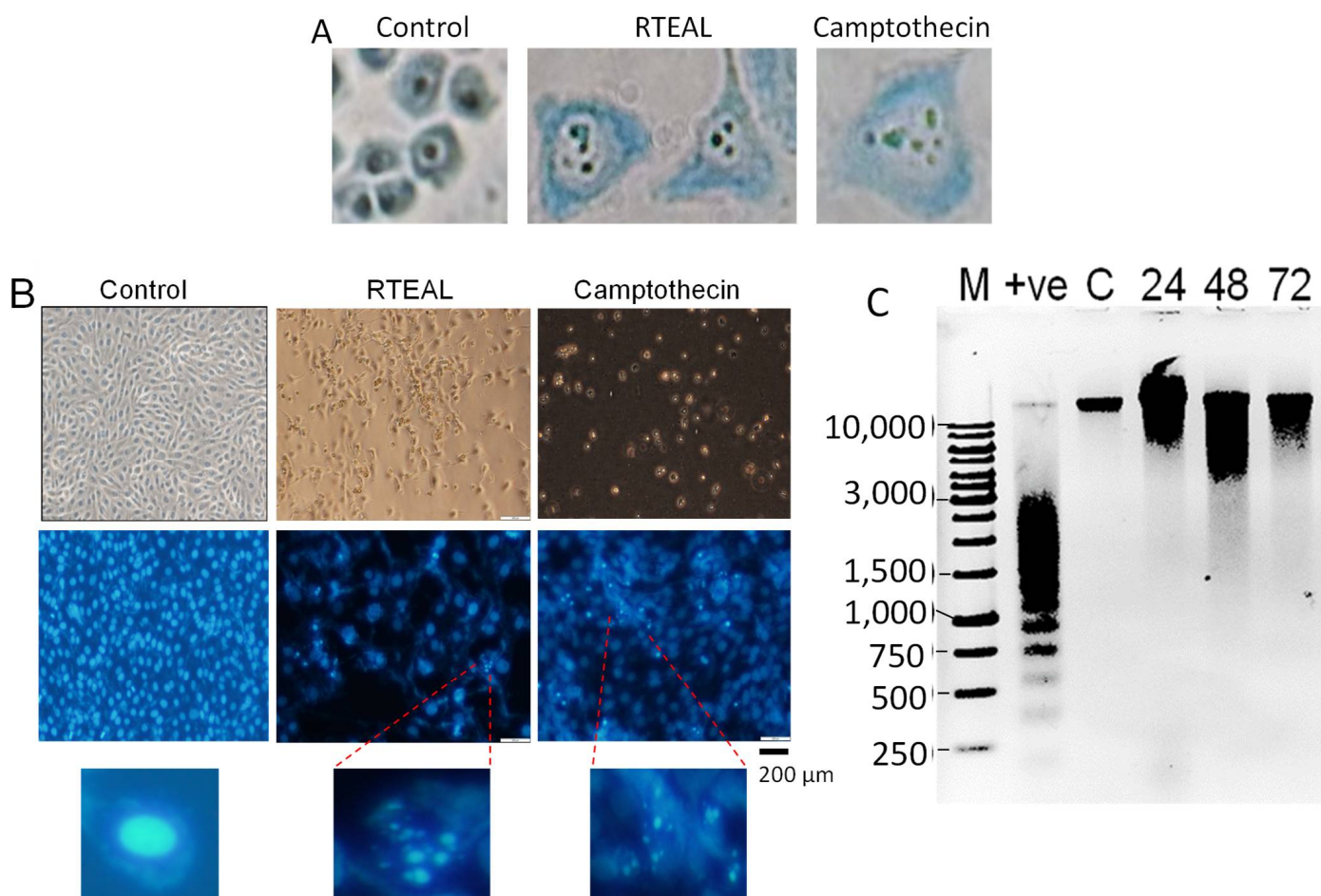


**Figure 2.** Effects of RTEAL on cell morphology and DNA fragmentation. MCF-7 cells were treated with 28  $\mu$ g/mL and stained with methylene blue (**A**) and DAPI (**B**). Morphological changes were observed under a microscope with 400 $\times$  and 100 $\times$  magnification for (**A,B**), respectively. Intense DAPI-stained cells with condensed and fragmented nucleus were enlarged. (**C**) Agarose gel electrophoresis of extracted DNA. Lane M: 1 kB DNA marker; lane +ve: camptothecin treated cells provided by the kit and lane C: control treated with DMSO. Lanes 24, 48 and 72: samples treated for 24, 48 and 72 h, respectively.

### 3.3. Induction of Apoptosis

Annexin V/PI analysis revealed that RTEAL induces apoptosis in a time-dependent manner. A remarkable increase of apoptotic cells from 1.6% (24 h) to 48% (72 h) was observed in RTEAL-treated cells when compared to control (Figure 3A). However, the involvement of non-apoptotic cell death is also possible as there was a noticeable increase in dead cells after treatment. In addition, MCF-7 cells treated with RTEAL ( $31 \pm 1.18\%$ ) showed a significant decrease in mitochondrial membrane potential at 48 h (Figure 3B). The number of cells with mitochondrial defect decreased when the treatment was prolonged to 72 h. We also noticed an increase in BAX expression, which accompanied by a concomitant decrease in BCL-2 expression (Figure 4). The protein expressions of caspase 7 and 8 were also upregulated upon treatments when compared to the control (Figure 5).

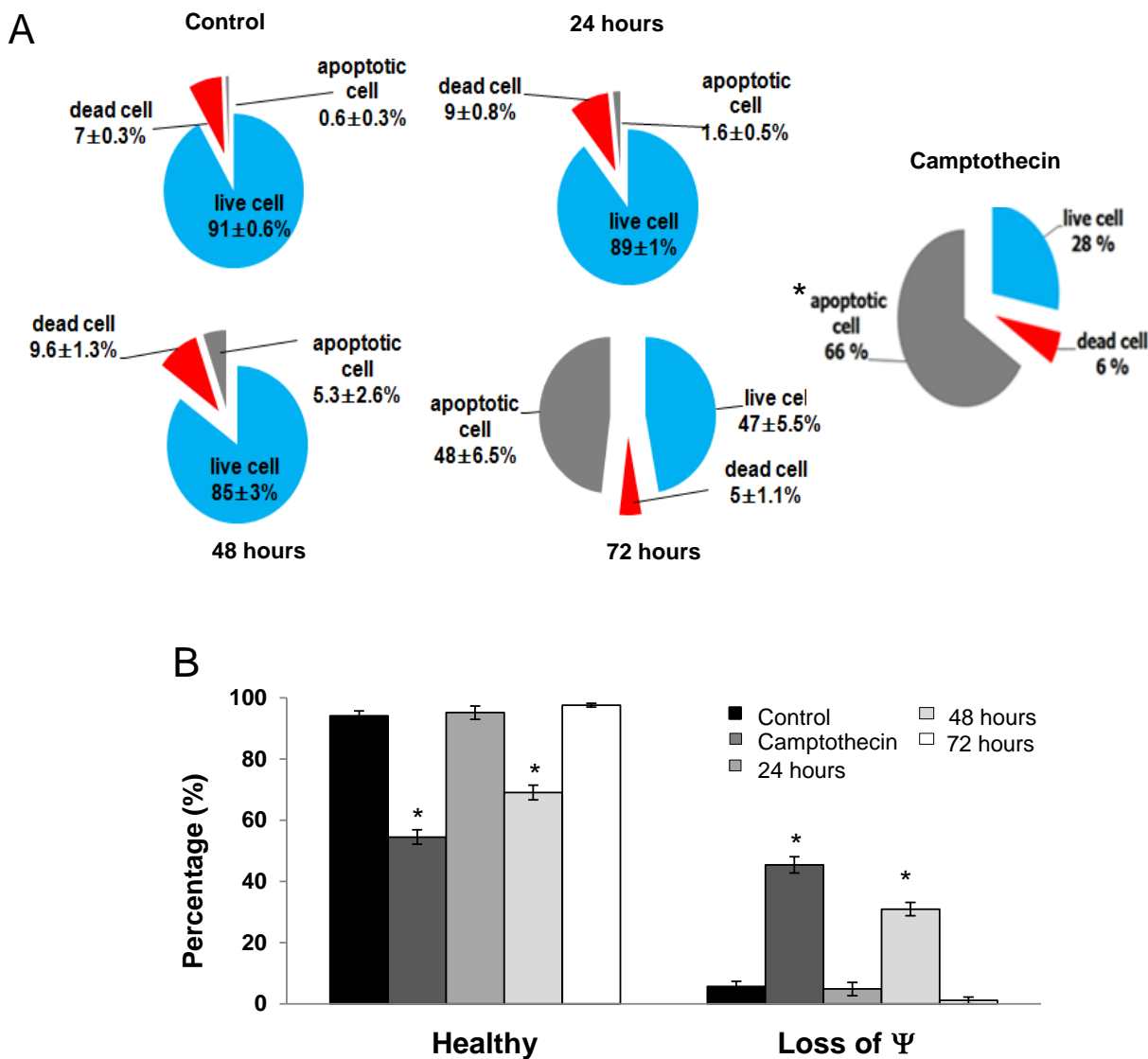


**Figure 3.** RTEAL induces apoptosis and mitochondrial dysfunction. Cells were treated with RTEAL at 28  $\mu$ g/mL for up to 72 h. (A) Distribution of apoptotic and dead cells. (B) Loss of mitochondrial membrane potential ( $\Psi$ ). Data were presented as mean  $\pm$  SEM of the three independent experiments. Asterisks indicate a significant difference (\*  $p < 0.05$ ) for each treatment was compared to the control cells.

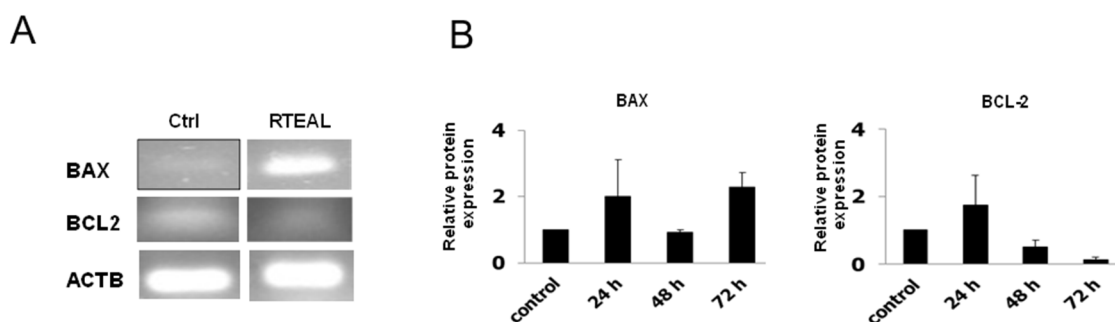


**Figure 4.** RTEAL alters the mRNA and protein expression of BCL-2 and BAX. MCF-7 cells were treated with 28  $\mu$ g/mL of RTEAL for 24, 48 and 72 h. (A) RT-PCR results of cells treated for 72 h. (B) The relative protein expression was quantified after normalizing with  $\beta$ -tubulin and presented as mean  $\pm$  SEM from three independent experiments.

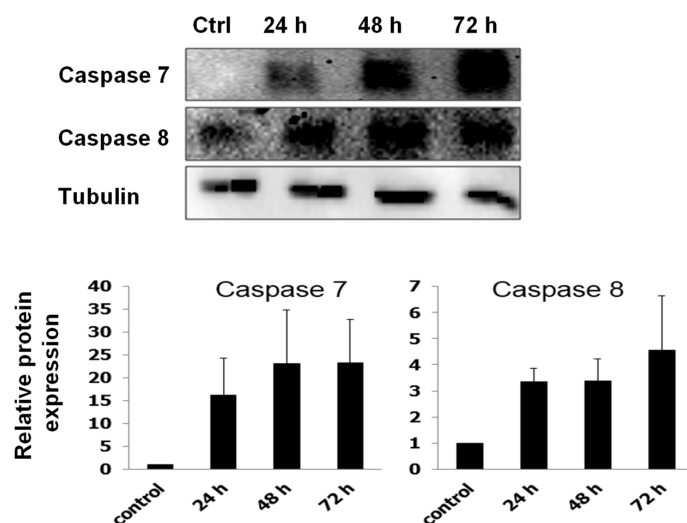


**Figure 5.** RTEAL increases the protein expression of caspases. MCF-7 cells were treated with 28  $\mu$ g/mL of RTEAL for 24, 48 and 72 h. Representative Western blot and relative protein expression was quantified after normalizing with  $\beta$ -tubulin. Data were presented as mean  $\pm$  SEM from three independent experiments.

### 3.4. Perturbation of Cell Cycle

As depicted in Figure 6, cell cycle progression was perturbed at the S or G2/M phase depending on the concentration and duration of RTEAL treatment. Cells treated with different concentrations exhibited a significant cell arrest at the S phase, although the extent of perturbation is not apparent with the increased concentration. However, an increase of cell cycle arrest at G2/M and cell debris was noticeable at the concentration of 38  $\mu$ g/mL (Figure 6A). As shown by Western blot results, cell cycle arrest was evidenced with the dysregulation of cell cycle regulators. The decrease of cyclin E1 and A2 was concentration-dependent but not for CDK2 (Figure 6B). The expression of cyclin A2 was downregulated from 28  $\mu$ g/mL onward, while a decrease of cyclin E1 was only observed at 38  $\mu$ g/mL. For the time-course treatment, the appearance of apoptotic sub-population before G1 phase was only detected at 48 h when cells were treated with 18  $\mu$ g/mL of RTEAL (Figure 7). When the duration of treatment was prolonged to 72 h, more cells arrested at S phase when compared to the control. The cell cycle arrest after RTEAL treatment was also found to be time-course dependent.

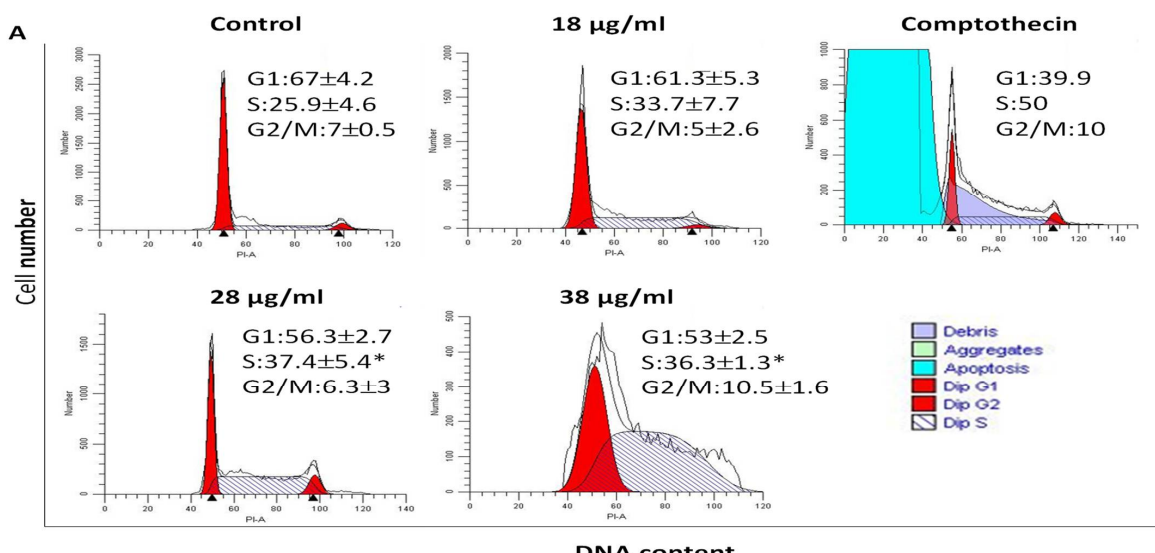


**Figure 6. Cont.**

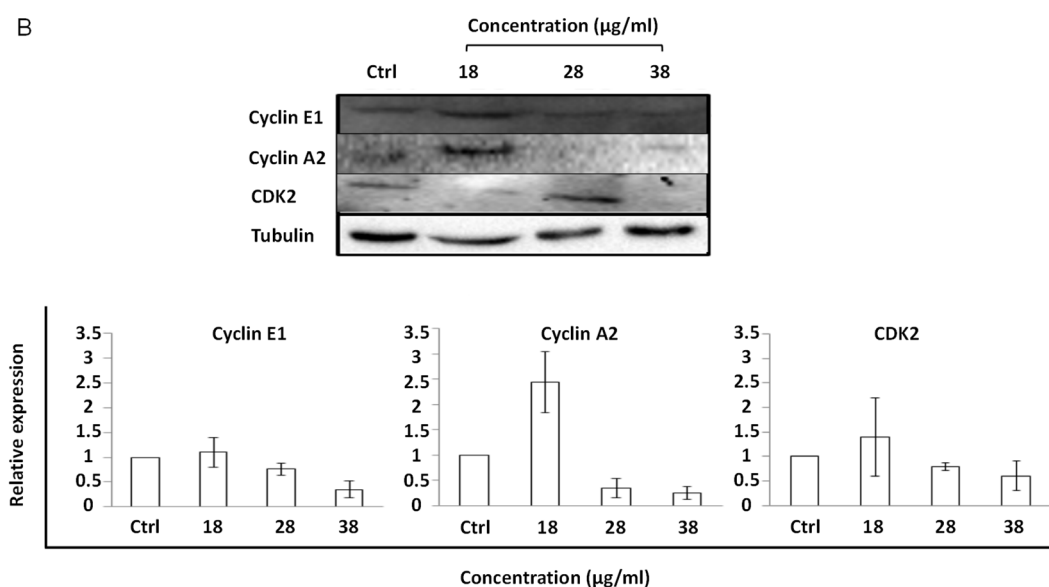


**Figure 6.** Cell cycle perturbation upon RTEAL treatment is concentration-dependent. (A) MCF-7 cells were treated with different concentrations of RTEAL as indicated for 72 h. (B) Representative Western blot and the relative protein expression of cyclins and CDK after normalizing with  $\beta$ -tubulin. Data were presented as mean  $\pm$  SEM from three independent experiments. Asterisks indicate a significant difference ( $* p < 0.05$ ) for each treatment was compared to the control cells.

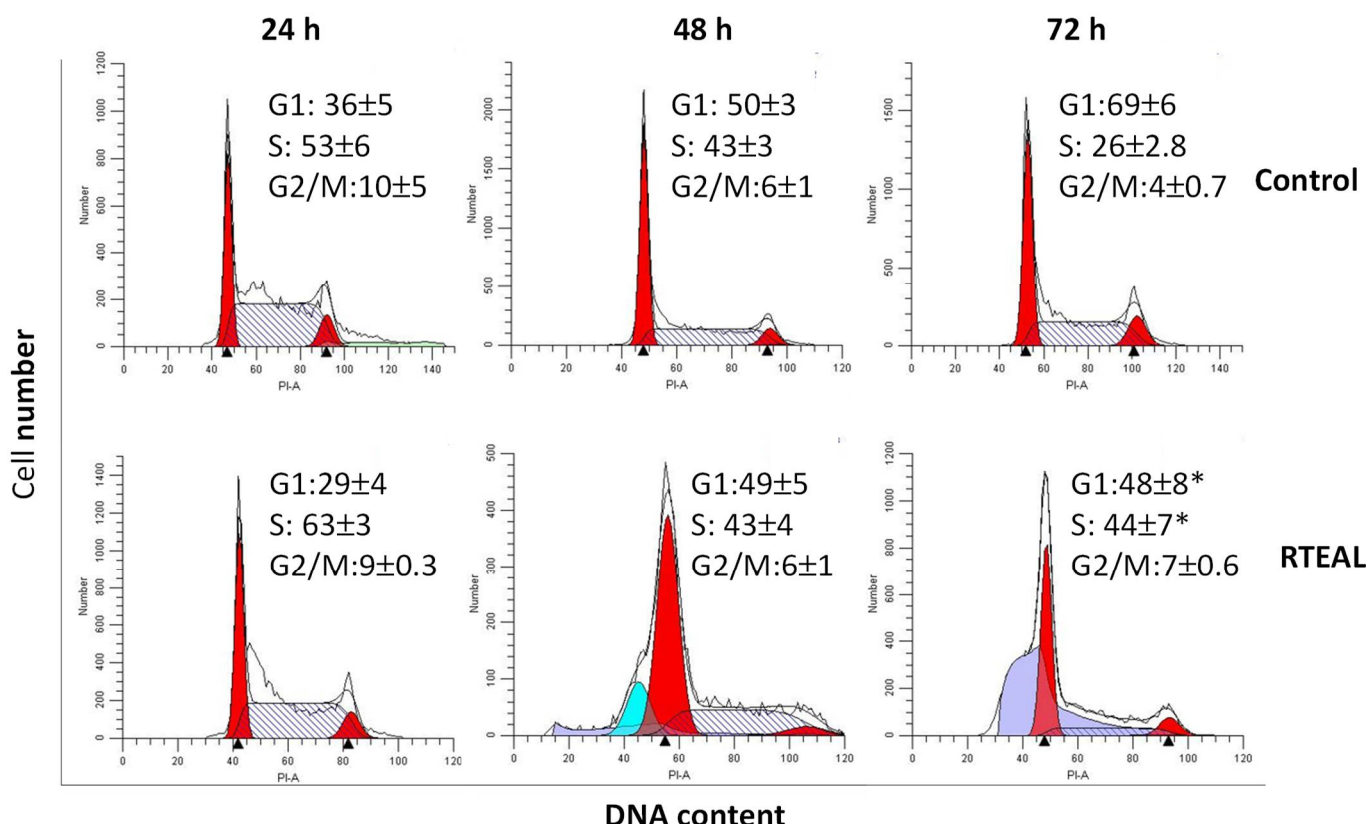


**Figure 7.** Time-dependent alteration in the cell cycle progression. MCF-7 cells were treated with 28  $\mu$ g/mL of RTEAL for 24, 48 and 72 h. Data were presented as mean  $\pm$  SEM of the three independent experiments. Asterisks indicate a significant difference ( $* p < 0.05$ ) for each treatment was compared to the control cells.

#### 4. Discussion

As we reported previously, *R. tuberosa* exerted an inhibitory effect on MCF-7 [24]. To understand its underlying mechanistic action, we fractionated its methanolic leaf extract through liquid-liquid partition and reassessed its efficacy on breast and normal cell lines. It is noticeable that the partitioned RTEAL showed better inhibitory activity than the crude extract from ethyl acetate leaf. Furthermore, RTEAL showed no cytotoxicity on the tested normal cells, MCF10A and NIH3T3 (Figure 1).

To investigate the mode of action executed by RTEAL, we first examined the morphological changes and the intactness of genomic DNA after treatment. By comparing the stained nuclear content of cells treated with camptothecin and RTEAL, the extract induces apoptotic cell death with no formation of DNA laddering (Figure 2). The presence of HMW DNA could have resulted from incomplete DNA cleavage in caspase 3-deficient cells such as MCF-7 [28,29]. In addition, caspase-independent DNA fragmentation could also occur via the activation of apoptosis-inducing factor (AIF), which induces DNA cleavage into high molecular mass fragments with no oligonucleosomal DNA fragmentation [30,31].

RTEAL-induced apoptotic cell death was further ascertained by the loss of mitochondrial membrane potential, elevated expression of BAX and caspases as well as downregulation of BCL-2. BCL-2 family proteins are key regulators that govern the permeability of the outer mitochondrial membrane. The binding of the anti-apoptotic protein, BCL-2 to pro-apoptotic proteins such as BAX causes the loss of mitochondrial membrane potential [32]. Thus, decreasing the expression of BCL-2 and upregulation of BAX expression are pivotal in promoting apoptosis. Our results also showed that the loss of the mitochondrial membrane integrity was not aligned with the increase of apoptotic cells as higher apoptotic cells was observed at 72 h while the decline of mitochondrial membrane potential was peak at 48 h (Figure 3). This is not uncommon because the characteristics of apoptosis are preceded by mitochondrial dysfunction, an initial event [33,34]. In addition, many studies have also demonstrated that mitochondrial dysfunction in apoptosis could be cell type and apoptotic stimuli dependent [35].

In term of caspases, we observed an increase in the expression of caspase 7 and 8 (Figure 5). It has been shown that the extrinsic apoptosis could be induced without activating the mitochondrial pathway via rapid activation of caspase 8 and the formation of death-inducing signaling complex (DISC) [36,37]. Recently, using CRISPR-based genome editing in human leukemia cells, caspase 8 and caspase 9 are both found to be activated during intrinsic and extrinsic apoptosis [36]. In addition, the presence of either caspase 3 or caspase 7 has been shown to activate apoptotic processes sufficiently [38]. Caspase 7 is an executioner caspase that redundant with caspase 3 although they are known to have distinct target genes [39,40]. In addition, the capability of plant extracts to modulate apoptosis in caspase 3-defective cells has been extensively studied [41,42].

Each phase of the cell cycle is controlled by a specific cyclin-CDK complex. For instance, CDK2 associates with cyclins such as cyclin E and cyclin A to regulate the entry from G1 phase to S phase and during S phase, respectively. On the other hand, the cyclin A-CDK1 complex promotes entry into mitosis [43,44]. Some drugs and natural compounds with the ability to target cell cycle regulators were found to increase the efficacy in current treatment [44–46]. We notice transient cell cycle arrests at S and G2/M phases at 24 h and 72 h, and the induction of apoptosis at 48 h upon RTEAL treatment (Figure 7). Increase of cell accumulation at G0/G1 and G2/M phase has been observed in HepG2 cells treated with methanolic leaf extract of *R. tuberosa* [25]. Cyclin E1 is highly expressed and associated with replication stress in estrogen-receptor positive (ER<sup>+</sup>) and triple-negative breast cancer, respectively, suggesting its potential as a therapeutic target [47,48]. Overexpression of cyclin A2 has resulted in poor prognosis in the early and metastatic stage of breast cancer. It plays an important role in regulating progesterone receptor (PR) target genes [49]. Downregulation of cyclin A2 and E1 could promote RTEAL-treated cells undergoing S and G2/M phase arrest (Figure 6). As perturbation of any phase of cell cycle progression will eventually lead to cell death, this explains the increase of cell debris at in cells treated with higher

concentration and longer duration of RTEAL. In contrast with in vivo conditions, apoptotic cells are engulfed by neighboring cells via phagocytosis [50]. However, we cannot rule out the possibility of other non-apoptotic cell death as well as any synergistic effect caused by bioactive compounds present in RTEAL extract.

In conclusions, these findings show that RTEAL induced apoptosis and cell cycle arrest by modulating BCL-2/BAX and CDK/cyclin proteins, respectively, suggesting its efficacy as a therapeutic agent for breast cancer.

**Author Contributions:** Supervision, conceptualization, P.L.T. and B.E.C.; methodology, P.L.T., B.E.C. and F.F.L.; investigation, F.F.L.; formal analysis, F.F.L.; validation, P.L.T. and F.F.L.; writing original draft preparation, F.F.L.; writing, review and editing, P.L.T. and B.E.C.; funding acquisition, P.L.T. and B.E.C. All authors have read and agreed to the published version of the manuscript.

**Funding:** This work was supported by Universiti Malaysia Sabah (SBK0053-SG-2013) and the Ministry of Higher Education (FRG0360-SG-2/2013).

**Institutional Review Board Statement:** Not applicable.

**Informed Consent Statement:** Not applicable.

**Data Availability Statement:** Data are available upon request.

**Acknowledgments:** Authors thank Universiti Malaysia Sabah for providing funding for the publication of this manuscript.

**Conflicts of Interest:** The authors declare that there was no conflict of interest.

## References

- Pucci, C.; Martinelli, C.; Ciofani, G. Innovative approaches for cancer treatment: Current perspectives and new challenges. *Ecancermedicalscience* **2019**, *13*, 961. [[CrossRef](#)] [[PubMed](#)]
- World Health Organization. Cancer. 2022. Available online: <https://www.who.int/news-room/fact-sheets/detail/cancer> (accessed on 29 April 2022).
- Turner, K.M.; Yeo, S.K.; Holm, T.M.; Shaughnessy, E.; Guan, J.L. Heterogeneity within molecular subtypes of breast cancer. *Am. J. Physiol.-Cell Physiol.* **2021**, *321*, C343–C354. [[CrossRef](#)] [[PubMed](#)]
- Testa, U.; Castelli, G.; Pelosi, E. Breast cancer: A molecularly heterogenous disease needing subtype-specific treatments. *Med. Sci.* **2020**, *8*, 18. [[CrossRef](#)]
- Nouri, Z.; Fakhri, S.; Nouri, K.; Wallace, C.E.; Farzaei, M.H.; Bishayee, A. Targeting multiple signaling pathways in cancer: The rutin therapeutic approach. *Cancers* **2020**, *12*, 2276. [[CrossRef](#)]
- De Melo Gagliato, D.; Gonzalez-Angulo, A.M. Targeting multiple pathways in breast cancer. *Breast Cancer Manag.* **2014**, *3*, 87–101. [[CrossRef](#)]
- Jan, R.; Chaudhry, G.E. Understanding apoptosis and apoptotic pathways targeted cancer therapeutics. *Adv. Pharm. Bull.* **2019**, *9*, 205–218. [[CrossRef](#)]
- Alimbetov, D.; Askarova, S.; Umbayev, B.; Davis, T.; Kipling, D. Pharmacological targeting of cell cycle, apoptotic and cell adhesion signaling pathways implicated in chemoresistance of cancer Cells. *Int. J. Mol. Sci.* **2018**, *19*, 1690. [[CrossRef](#)]
- Haque, A.; Brazeau, D.; Amin, A.R. Perspectives on natural compounds in chemoprevention and treatment of cancer: An update with new promising compounds. *Eur. J. Cancer* **2021**, *149*, 165–183. [[CrossRef](#)]
- Newman, D.J.; Cragg, G.M. Natural products as sources of new drugs over the nearly four decades from 01/1981 to 09/2019. *J. Nat. Prod.* **2020**, *83*, 770–803. [[CrossRef](#)]
- Sun, L.R.; Zhou, W.; Zhang, H.M.; Guo, Q.S.; Yang, W.; Li, B.J.; Sun, Z.H.; Gao, S.H.; Cui, R.J. Modulation of multiple signaling pathways of the plant-derived natural products in cancer. *Front. Oncol.* **2019**, *9*, 1153. [[CrossRef](#)]
- Yuan, L.; Cai, Y.; Zhang, L.; Liu, S.; Li, P.; Li, X. Promoting apoptosis, a promising way to treat breast cancer with natural products: A comprehensive review. *Front. Pharmacol.* **2022**, *12*, 801662. [[CrossRef](#)] [[PubMed](#)]
- Arirudran, B.; Saraswathy, A.; Krishnamurthy, V. Pharmacognostic and preliminary phytochemical studies on *Ruellia tuberosa* L. (Whole plant). *Pharmacogn. J.* **2011**, *3*, 29–34. [[CrossRef](#)]
- Chen, F.A.; Wu, A.B.; Shieh, P.; Kuo, D.H.; Hsieh, C.Y. Evaluation of the antioxidant activity of *Ruellia tuberosa*. *Food Chem.* **2006**, *94*, 14–18. [[CrossRef](#)]
- Chothani, D.L.; Mishra, H. In vitro anti-oxidant activity of *Ruellia tuberosa* root extracts. *Free. Radic. Antioxid.* **2012**, *2*, 38–44. [[CrossRef](#)]
- Afzal, K.; Uzair, M.; Chaudhary, B.A.; Ahmad, A.; Afzal, S.; Saadullah, M. Genus *Ruellia*: Pharmacological and phytochemical importance in ethnopharmacology. *Acta Pol. Pharm.-Drug Res.* **2015**, *72*, 821–827.

17. Alam, M.A.; Subhan, N.; Awal, M.A.; Alam, M.S.; Sarder, M.; Nahar, L.; Sarker, S.D. Atinociceptive and anti-inflammatory properties of *Ruellia tuberosa*. *Pharma. Biol.* **2009**, *47*, 209–214. [CrossRef]
18. Jiorry, J.R.S.; Cheong, B.E. Metabolic fingerprinting of Sabah *Ruellia tuberosa* plant extracts for the identification of potential anti-cancer compounds. *Short Commun. Biotech.* **2017**, *4*, 75–87. Available online: <https://www.ums.edu.my/ibpv2/files/Metabolic-Fingerprinting-of-Sabah-Ruellia-tuberosa-Plant-Extracts-for-the-Identification-of-Potential-Anticancer-Compounds.pdf> (accessed on 3 July 2022).
19. Lin, C.-F.; Huang, Y.-L.; Cheng, L.-Y.; Sheu, S.-J.; Chen, C.-C. Bioactive flavonoids from *Ruellia tuberosa*. *J. Chin. Med.* **2006**, *17*, 103–109.
20. Mohan, V.; Rajendrakumar, N.; Vasantha, K. GC-MS Analysis of bioactive components of tubers of *Ruellia tuberosa* L. (Acanthaceae). *Am. J. Phytomed. Clin. Ther.* **2014**, *2*, 209–216.
21. Sánchez-Quesada, C.; Gutiérrez-Santiago, F.; Rodríguez-García, C.; Gaforio, J.J. Synergistic effect of squalene and hydroxytyrosol on highly invasive MDA-MB-231 breast cancer cells. *Nutrients* **2022**, *14*, 255. [CrossRef]
22. Pitchai, D.; Roy, A.; Ignatius, C. In vitro evaluation of anticancer potentials of lupeol isolated from *Elephantopus scaber* L. on MCF-7 cell line. *J. Adv. Pharm. Technol. Res.* **2014**, *5*, 179–184. [CrossRef] [PubMed]
23. Zhang, X.; Gao, Z.; Chen, K.; Zhuo, Q.; Chen, M.; Wang, J.; Lai, X.; Wang, L. Lupeol inhibits the proliferation and migration of MDA-MB-231 breast cancer cells via a novel crosstalk mechanism between autophagy and the EMT. *Food Funct.* **2022**, *13*, 4967. [CrossRef] [PubMed]
24. Cheong, B.E.; Waslim, M.Z.; Lem, F.F.; Teoh, P.L. Antioxidant and anti-proliferative activities of Sabah *Ruellia tuberosa*. *J. Appl. Pharma. Sci.* **2013**, *3*, 20–24. [CrossRef]
25. Dey, S.; Roy, S.; Deb, N.; Kumar Sen, K.; Besra, S.E. Anticarcinogenic activity of *Ruellia tuberosa* L. (Acanthaceae) leaf extract on hepatoma cell line and increased superoxide dismutase activity on macrophage cell lysate. *Int. J. Pharm. Pharm. Sci.* **2015**, *5*, 854–861.
26. Teoh, P.L.; Cheng, A.Y.F.; Liau, M.; Lem, F.F.; Kaling, G.P.; Chua, F.N.; Cheong, B.E. Chemical composition and cytotoxic properties of *Clinacanthus nutans* root extracts. *Pharm. Biol.* **2017**, *55*, 394–401. [CrossRef]
27. Teoh, P.L.; Liau, M.; Cheong, B.E. *Phyla nodiflora* L. extracts induce apoptosis and cell cycle arrest in human breast cancer cell line, MCF-7. *Nutr. Cancer* **2019**, *71*, 668–675. [CrossRef]
28. Walker, P.R.; Leblanc, J.; Carson, C.; Ribecco, M.; Sikorska, M. Neither caspase-3 nor DNA fragmentation factor is required for high molecular weight DNA degradation in apoptosis. *Ann. N. Y. Acad. Sci.* **1999**, *887*, 48–59. [CrossRef]
29. Iglesias-Guimaraes, V.; Gil-Guiñon, E.; Gabernet, G.; García-Belinchón, M.; Sánchez-Osuna, M.; Casanelles, E.; Comella, J.X.; Yuste, V.J. Apoptotic DNA degradation into oligonucleosomal fragments, but not apoptotic nuclear morphology, relies on a cytosolic pool of DFF40/CAD endonuclease. *J. Biol. Chem.* **2012**, *287*, 7766–7779. [CrossRef]
30. Susin, S.A.; Lorenzo, H.K.; Zamzami, N.; Marzo, I.; Snow, B.E.; Brothers, G.M.; Mangion, J.; Jacotot, E.; Costantini, P.; Loeffler, M.; et al. Molecular characterization of mitochondrial apoptosis-inducing factor. *Nature* **1999**, *397*, 441–446. [CrossRef]
31. Kitazumi, I.; Tsukahara, M. Regulation of DNA fragmentation: The role of caspases and phosphorylation. *FEBS J.* **2011**, *278*, 427–441. [CrossRef]
32. Lalier, L.; Vallette, F.; Manon, S. Bcl-2 family members and the mitochondrial import machineries: The roads to death. *Biomolecules* **2022**, *12*, 162. [CrossRef] [PubMed]
33. Shimizu, S.; Eguchi, Y.; Kamiike, W.; Funahashi, Y.; Mignon, A.; Lacronique, V.; Matsuda, H.; Tsujimoto, Y. Bcl-2 prevents apoptotic mitochondrial dysfunction by regulating proton flux. *Proc. Natl. Acad. Sci. USA* **1998**, *95*, 1455–1459. [CrossRef] [PubMed]
34. Zuo, Y.; Hu, J.; Xu, X.; Gao, X.; Wang, Y.; Zhu, S. Sodium azide induces mitochondria-mediated apoptosis in PC12 cells through Pgc-1 $\alpha$ -associated signaling pathway. *Mol. Med. Rep.* **2019**, *19*, 2211–2219. [CrossRef] [PubMed]
35. Ly, J.D.; Grubb, D.R.; Lawen, A. The mitochondrial membrane potential ( $\Delta\psi_m$ ) in apoptosis; an update. *Apoptosis* **2003**, *8*, 115–128. [CrossRef]
36. Kantari, C.; Walczak, H. Caspase-8 and bid: Caught in the act between death receptors and mitochondria. *Biochim. Biophys. Acta (BBA)-Mol. Cell Res.* **2011**, *1813*, 558–563. [CrossRef]
37. Wu, Y.; Zhao, D.; Zhuang, J.; Zhang, F.; Xu, C. Caspase-8 and caspase-9 functioned differently at different stages of the cyclic stretch-induced apoptosis in human periodontal ligament cells. *PLoS ONE* **2016**, *11*, e0168268. [CrossRef]
38. McComb, S.; Chan, P.K.; Guinot, A.; Hartmannsdottir, H.; Jenni, S.; Dobay, M.P.; Bourquin, J.P.; Bornhauser, B.C. Efficient apoptosis requires feedback amplification of upstream apoptotic signals by effector caspase-3 or -7. *Sci. Adv.* **2019**, *5*, eaau9433. [CrossRef]
39. Walsh, J.G.; Cullen, S.P.; Sheridan, C.; Lüthi, A.U.; Gerner, C.; Martin, S.J. Executioner caspase-3 and caspase-7 are functionally distinct proteases. *Proc. Natl. Acad. Sci. USA* **2008**, *105*, 12815–12819. [CrossRef]
40. Lamkanfi, M.; Kanneganti, T.D. Caspase-7: A protease involved in apoptosis and inflammation. *Int. J. Biochem. Cell Biol.* **2010**, *42*, 21–24. [CrossRef]
41. Foo, J.B.; Yazan, L.S.; Tor, Y.S.; Armania, N.; Ismail, N.; Imam, M.U.; Yeap, S.K.; Cheah, Y.K.; Abdullah, R.; Ismail, M. Induction of cell cycle arrest and apoptosis in caspase-3 deficient MCF-7 cells by *Dillenia suffruticosa* root extract via multiple signaling pathways. *BMC Complement. Altern. Med.* **2014**, *14*, 197. [CrossRef]

42. Sakle, N.S.; More, S.A.; Mokale, S.N. Chemomodulatory effects of *Alysicarpus vaginalis* extract via mitochondria-dependent apoptosis and necroptosis in breast cancer. *Nutr. Cancer* **2020**, *72*, 1243–1253. [[CrossRef](#)] [[PubMed](#)]
43. Lim, S.; Kaldis, P. Cdks, cyclins and CKIs: Roles beyond cell cycle regulation. *Development* **2013**, *140*, 3079–3093. [[CrossRef](#)] [[PubMed](#)]
44. Ding, L.; Cao, J.; Lin, W.; Chen, H.; Xiong, X.; Ao, H.; Yu, M.; Lin, J.; Cui, Q. The roles of cyclin-dependent kinases in cell-cycle progression and therapeutic strategies in human breast cancer. *Int. J. Mol. Sci.* **2020**, *21*, 1960. [[CrossRef](#)]
45. Bailon-Moscoso, N.; Cevallos-Solorzano, G.; Romero-Benavides, J.C.; Orellana, M.I.R. Natural compounds as modulators of cell cycle arrest: Application for anticancer chemotherapies. *Curr. Genom.* **2017**, *18*, 106–131. [[CrossRef](#)] [[PubMed](#)]
46. Thu, K.L.; Soria-Bretones, I.; Mak, T.W.; Cescon, D.W. Targeting the cell cycle in breast cancer: Towards the next phase. *Cell Cycle* **2018**, *17*, 1871–1885. [[CrossRef](#)] [[PubMed](#)]
47. Milioli, H.H.; Alexandrou, S.; Lim, E.; Caldon, C.E. Cyclin E1 and cyclin E2 in ER+ breast cancer: Prospects as biomarkers and therapeutic targets. *Endocr.-Relat. Cancer* **2020**, *27*, R93–R112. [[CrossRef](#)]
48. Guerrero Llobet, S.; van der Vegt, B.; Jongeneel, E.; Bense, R.D.; Zwager, M.C.; Schröder, C.P.; Everts, M.; Fehrmann, R.S.; de Bock, G.H.; van Vugt, M.A. Cyclin E expression is associated with high levels of replication stress in triple-negative breast cancer. *NPJ Breast Cancer* **2020**, *6*, 40. [[CrossRef](#)]
49. Moore, N.L.; Edwards, D.P.; Weigel, N.L. Cyclin A2 and its associated kinase activity are required for optimal induction of progesterone receptor target genes in breast cancer cells. *J. Steroid Biochem. Mol. Biol.* **2014**, *144 Pt B*, 471–482. [[CrossRef](#)]
50. Gordon, S.; Plüddemann, A. Macrophage clearance of apoptotic cells: A critical assessment. *Front. Immunol.* **2018**, *9*, 127. [[CrossRef](#)]